

Monte Carlo simulation of silicon atomic displacement and amorphization induced by ion implantation

Luis Jou García,¹ Yoko Kawamura,¹ Masashi Uematsu,¹ Jesús M. Hernández-Mangas,² and Kohei M. Itoh^{1,a)}

¹*School of Fundamental Science and Technology, Keio University, 3-14-1 Hiyoshi, Kohoku-ku, Yokohama, 223-8522, Japan*

²*Departamento de Electricidad y Electrónica, Universidad de Valladolid, E.T.S.I. Telecomunicación, 47011 Valladolid, Spain*

(Received 24 February 2011; accepted 14 April 2011; published online 20 June 2011)

The amorphization of silicon due to atomic displacement during ion implantation has been simulated. A model based on Monte Carlo calculation reproduces very well the depth profile of atomic mixing and displacement length of host silicon atoms reported by previous experiments. The critical displacement in the depth direction for amorphization has been determined to be 5 Å. This average threshold value is shown to be universal for identification of amorphous regions in silicon for a wide range of implantation conditions involving different doping species, acceleration energies, and doses.

© 2011 American Institute of Physics. [doi:10.1063/1.3592256]

I. INTRODUCTION

Amorphization of silicon during ion implantation is an active area of research because it is strongly related to the electrical activation of implanted dopants in the source and drain regions of silicon CMOS transistors. Amorphization prevents ion channeling and, hence, is effective to achieve ultra-shallow doping. Moreover, an amorphous region can be annealed out easily to form the low defect density and highly activated source and drain regions. However, end-of-range (EOR) defects are known to accumulate in the vicinity of the amorphous/crystalline (a/c) interface.¹ These defects are responsible for transient anomalies of the dopant diffusion and current leakage. Therefore it is critical to establish a model to accurately predict the position of the a/c interface and develop methods to suppress these undesirable effects.

Several models have been proposed to unravel the mechanisms of amorphization in semiconductors.² They can be classified depending on whether they rely on the energy threshold,³⁻⁵ overlapping damage,^{6,7} or nucleation-based approach.⁸⁻¹⁰ However, all of these methods require employment of look-up parameters tabulated for the variety of implantation conditions. This work, on the other hand, presents a universal model that does not require adjustment of parameters to predict the position of the a/c interface for a wide range of implanted species/energy/dose combinations. The model justifies the importance and applicability of the new length scale, *the average atomic displacement*, that was found empirically to predict the position of the a/c interfaces.^{11,12}

II. SIMULATION DETAILS

Our calculation is carried out in three steps. First, we obtain and normalize the damage profile subsequent to an ion-implantation process in pure crystalline silicon. Second, we extrapolate this normalized profile into an atomic mixing

profile the validity of which is justified by the excellent agreement with experiments of Shimizu *et al.*¹¹ Third, the mixing profile is convoluted with Gaussian distributions in order to obtain the measure of the local displacement for each atom. Finally, the average displacement of the host silicon atoms in the depth direction is obtained. Our calculation is shown to be fully consistent with the empirical results shown in Refs. 11 and 12. Furthermore, the existence of the critical average displacement 5 Å in the depth direction is established and this defines accurately the position of the a/c interface reported in the literature for a wide range of doses, energies, and implanted species.

A. Vacancy generation

As the first step for our calculations, the concentration profile of vacancies as a result of implantation is obtained by the ION IMPLANT SIMULATOR (IIS)¹³ software developed by the University of Valladolid. The IIS has been shown to accurately reproduce the implantation of dopants into semiconductors with only a small set of input parameters. This simulator includes a Binary Collision Approximation (BCA)¹⁴ module to generate the cascades of defects produced when an energetic ion is accelerated and implanted into the crystalline material. The most recent version of the IIS code allows us to extract the entire set of raw data (species, xyz position) for interstitials and vacancies. Based on the vacancy distribution, calculations to obtain the displacement and amorphization are performed. The interstitial profile can be ignored because the vacancy in the BCA simulator represents the original location of each *moved atom* to deduce the displacement from the recoil.

The number of point defects originated per cascade depends on the implanted species and acceleration energy. However, because each cascade generates thousands of point defects, we consider 100 cascades with more than 100000 vacancies overall; a number large enough to assure the statistical accuracy. Our calculation results are compared directly

^{a)}Author to whom correspondence should be addressed. Electronic mail: kitoh@appi.keio.ac.jp.

to the host silicon displacement and depth of amorphization obtained quantitatively by the dopant implantation into silicon isotopes heterostructures.¹¹

The vacancy profile obtained by the BCA calculation is normalized to make it independent of the size of the grid employed to evaluate the number of cascades simulated. Thus the normalized profile $V_{Asi}^*(x)$ is given by

$$V_{Asi}^*(x) = \frac{V_{Asi}(x)}{V_{Asi}^T d_x}, \quad (1)$$

where $V_{Asi}(x)/d_x$ is the number of vacancies of Asi isotope per unit length formed during the cascades, d_x is the grid spacing employed in the calculation, and V_{Asi}^T is the total sum of vacancies that normalize $V_{Asi}(x)/d_x$. The resulting value $V_{Asi}^*(x)$ is then not proportional to the number of simulated cascades and, hence, can be regarded as a depth-dependent statistical distribution of the displacement induced to the atoms in the single crystal.

B. Atomic Mixing

The next step is to obtain the degree of atomic mixing from the statistical displacement distribution in Eq. (1). The present calculation that reproduces the mixing of a bulk material made from one or two different silicon isotopes can be extended easily to a situation with three or more species.

The mixing proceeds rapidly when two kinds of species to be mixed are spatially separated, and slows down as the degree of mixing is increased. Therefore, we employ the following equations to represent the rapid mixing linearly and the saturating mixing sublinearly:

$$C_{Asi}(x) = m_{Asi}^F - (m_{Asi}^F - C_{Asi}^0(x))e^{-FV_{Asi}^*(x)}, \quad (2)$$

$$C_{BSi}(x) = 1 - C_{Asi}(x), \quad (3)$$

where $C_{Asi}^0(x)$ and $C_{Asi}(x)$ are the depth-dependent isotopic fraction of Asi in the silicon bulk before and after implantation, m_{Asi}^F is the fully mixed fraction (constant and average fraction of Asi along the whole bulk), and $V_{Asi}^*(x)$ is the normalized value of vacancies placed at the depth between x and $x + d_x$. F is the factor defined as:

$$F = F_0 \frac{D}{D_0} \frac{E}{E_0}. \quad (4)$$

F is linear to the implantation dose D and energy E of the ions since D and E would increase the displacement distance of the recoiled atoms. F_0 , D_0 , and E_0 are constants that could be merged, but are separated in this work because F_0 can be obtained by fitting the results of implantation with reference dose D_0 and reference energy E_0 .

A quantitative verification of our simulated mixing profiles at this point is obtained by direct comparison with experimentally obtained mixing profiles after implantations of arsenic into silicon isotope hetero-structures.¹¹ Here the degree of mixing was deduced from the depth profile of the displaced silicon isotopes revealed by secondary ion mass spectrometry (SIMS).¹¹ In order to directly compare with the SIMS profile, it was necessary to smear out our calculation

results appropriately to account for unavoidable artifact associated with the SIMS measurement. Here an established method referred to as the MRI (Mixing, Roughness and Information-Depth) model is employed to complete the task.¹⁵ The procedure of the MRI analysis is described in Ref. 11. Figure 1 shows the comparison of the calculated isotope profiles with the SIMS results. Remarkable agreements between the present calculation and experiments have been obtained for the entire depth of two implantation energies (25 and 60 keV) and three different doses (1×10^{14} , 3×10^{14} , and

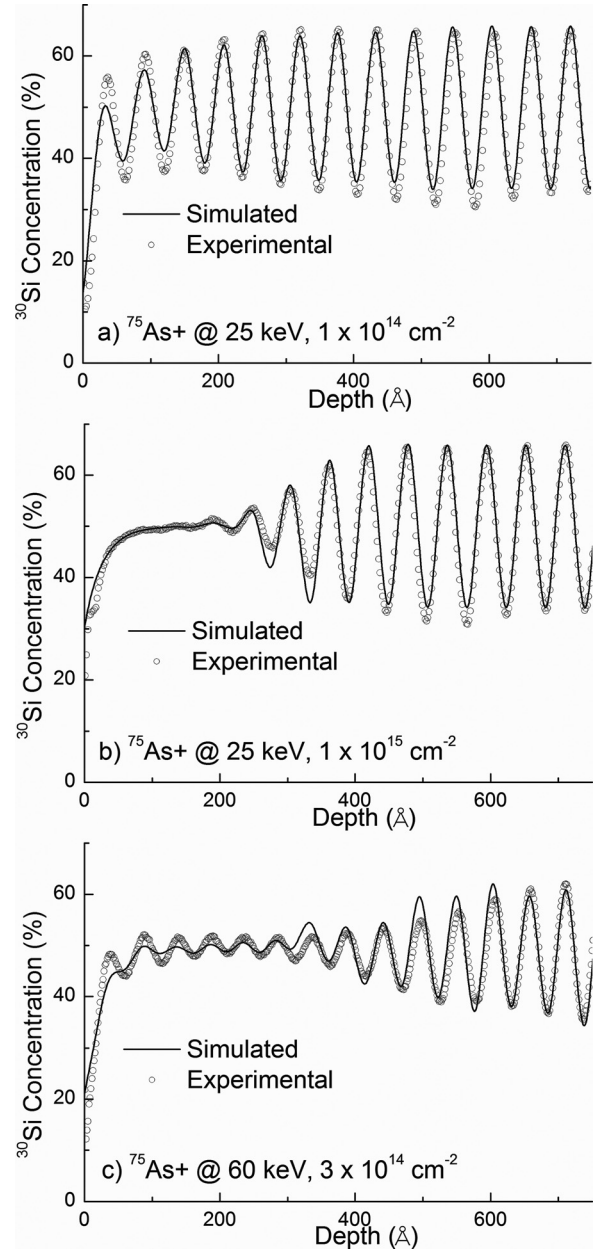


FIG. 1. Depth profiles of ^{30}Si in a $^{28}\text{Si}/^{30}\text{Si}$ isotope superlattice subsequent to $^{75}\text{As}^+$ ion implantation. Round symbols represent the SIMS result of Shimizu *et al.* (Ref. 11) and thin solid lines are the outcome of our simulation with the MRI (Ref. 15) rectifications applied to reproduce the SIMS artifacts (MRI parameters used are $w = 2.6$ nm (atomic mixing) and $s = 0.7$ nm (surface roughness), as described in Ref. 11). Implantation conditions are $1 \times 10^{14} \text{ cm}^{-2}$ at 25 keV (a), $1 \times 10^{15} \text{ cm}^{-2}$ at 25 keV (b), and $3 \times 10^{14} \text{ cm}^{-2}$ at 60 keV (c).

$1 \times 10^{15} \text{cm}^{-2}$). Hence, the validity of our mixing model is confirmed.

C. Average Atomic Displacement

The last stage of this simulation is to obtain the atomic displacement $D(x_i)$, which is defined as the average displacement distance between their original depth positions and displaced depth positions.

It is known that the depth distribution of the concentration of an implanted species can be approximated by a Gaussian distribution.¹⁶ This macroscopic Gaussian distribution is composed of many Gaussian broadenings arising from a large number of subcascades, i.e., host-silicon displacement can be identified by the local Gaussian broadening as a function of the depth. Therefore, we apply Gaussian broadening to the profile of degree of mixing in the bulk, $C^f(x_j)$, which corresponds to the fraction of moved atoms at the depth step $x_j = j \times d_x$. This profile ranges from 0% for undamaged areas to 100% in fully mixed regions and is obtained from Eq. (2) using parameters $C_{\text{Asi}}^0(x) = 0$ and $m_{\text{Asi}}^F = 1$. Calculation of the average displacement $D(x_i)$ for atoms moved to depth x_i is performed by the following discrete convolution;

$$D(x_i) = \sum_j \frac{1}{2} C^f(x_j) |x_i - x_j| g(x_i - x_j) d_x. \quad (5)$$

Here small enough steps of the order of 1 Å are adopted to minimize the effect of not using the integral. $|x_i - x_j|$ is the displaced distance based on the Gaussian distribution centered at x_j and with a standard deviation of $\sigma = 50 \text{Å}$,

$$g(x) = \frac{1}{\sigma\sqrt{2\pi}} \exp\left(-\frac{x^2}{2\sigma^2}\right). \quad (6)$$

The value of σ is the only adjustable parameter in Eq. (5) and, also, in the whole simulation procedure, which must be determined uniquely as an intrinsic value for the silicon single crystal as it represents the physical measure of how easily host crystal atoms are displaced as a result of implantations. It should be stressed that the value of σ is fixed for silicon and does not depend on the implantation conditions.

III. RESULTS AND DISCUSSION

Figure 2 shows the simulated displacement profiles $D(x_i)$ under the same conditions and configuration as in Fig. 1, i.e., $^{75}\text{As}^+$ implanted with 25 or 60 keV with doses of 1×10^{14} , 3×10^{14} , or $1 \times 10^{15} \text{cm}^{-2}$. It also shows the cross-sectional transmission electron microscope (XTEM) images of experimental samples taken from Ref. 11. Our goal is to find the relation between these two results to determine the critical displacement for amorphization of silicon. The critical displacement exists clearly; the matrix becomes amorphous when the displacement is larger than 5 Å and remains single crystalline when smaller than 5 Å. Therefore, the amorphous/crystalline (a/c) interfaces situate at depths that have the critical displacement 5 Å. The calculated and experimental profiles share similar characteristics; having the maximum peak placed slightly deeper than the region of maximum damage, having similar slopes, etc. They also find

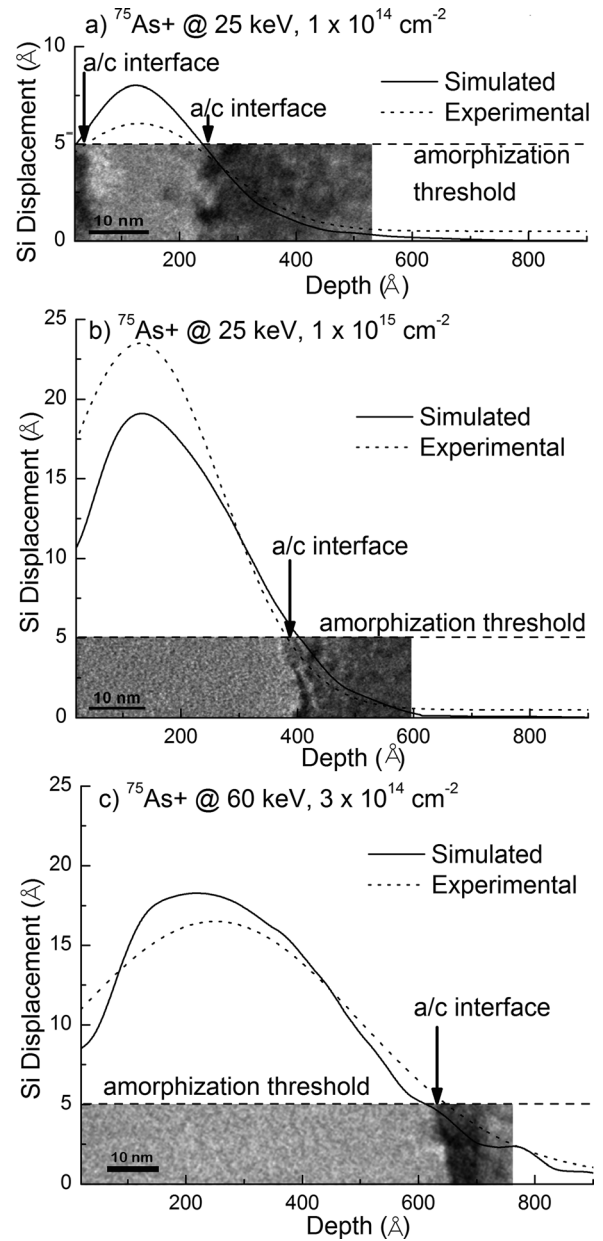


FIG. 2. Simulated and experimental depth dependences of the displacement of host Si atoms induced by implantation of $^{75}\text{As}^+$. Comparison with XTEM images of the experimental samples shows the existence of the amorphization threshold defined by 5 Å of the average atom displacement. Implantation conditions are $1 \times 10^{14} \text{cm}^{-2}$ at 25 keV (a), $1 \times 10^{15} \text{cm}^{-2}$ at 25 keV (b), and $3 \times 10^{14} \text{cm}^{-2}$ at 60 keV (c).

the same critical displacement 5 Å. The only noticeable discrepancy is the displacements in the shallow region where the Gaussian broadening of $\sigma = 50 \text{Å}$ may be too large to describe the phenomena near the surface. In this case, a non-symmetric broadening distribution would give more accurate results as compared to the Gaussian approach.

A further support of the validity of our method comes from the convergence of the calculated output to a constant and invariable value as the quality of the simulation is increased. This increase in quality is attained by raising the number of simulated cascades, hence reducing the shot noise, smoothing the vacancy profile, and getting an output less dependent on the random nature of the Monte Carlo simulation. Position of the a/c interface versus the number of

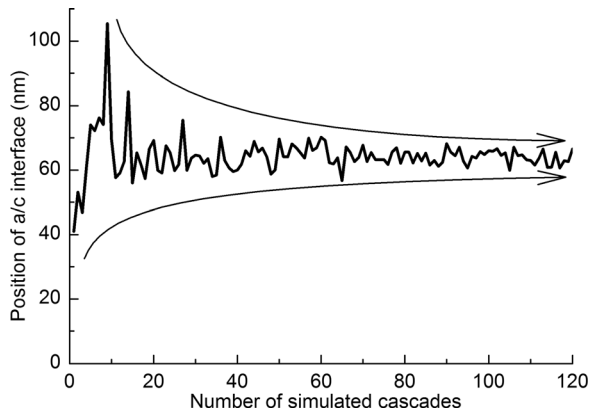


FIG. 3. Convergence of one of our Monte Carlo simulations for $^{75}\text{As}^+$ implantation at 60 keV and a dose of $3 \times 10^{14} \text{ cm}^{-2}$. The y axis represents the position of the a/c interface obtained by the criterion of 5 Å critical displacement with the number of cascades indicated by the x axis. (Arrow lines are guide to the eyes.)

simulated cascades is plotted in Fig. 3. The output value heavily fluctuates while the number of simulated cascades is less than 70, and beyond this point it converges.

Lastly, in order to show the universality of our calculation to obtain the position of the a/c interfaces, we have repeated the simulations using the same set of parameters for a wide variety of implantations conditions that have been employed to find the positions of the silicon a/c interfaces determined experimentally in the past.^{17–21} Using the critical displacement 5 Å, we obtain superb agreement of the a/c interface positions for a wide range of conditions including the dose, acceleration energy, and species of implanted ions, as shown in Fig. 4. Solid symbols represent the successful predictions where the calculated a/c interface position is

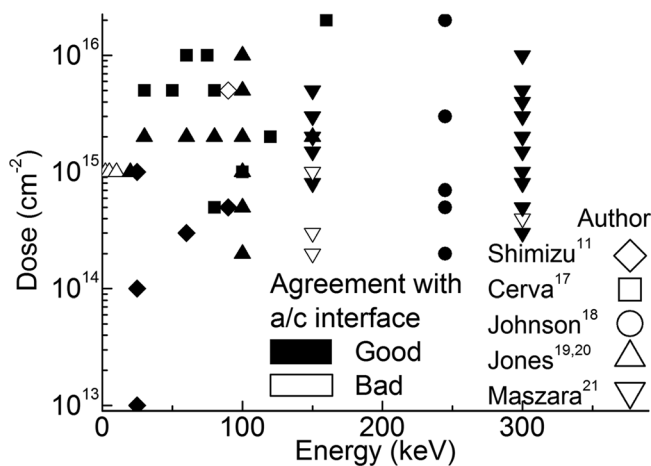


FIG. 4. Comparison of a/c interface positions in bulk silicon reported by a number of authors and obtained by our Monte Carlo simulation. Each point represents the experimentally reported position of the a/c interface. They are arranged horizontally depending on the acceleration of the ions with energies spanning from 2 to 300 keV, and vertically depending on the implanted dose extending from 1×10^{13} to $2 \times 10^{16} \text{ cm}^{-2}$. The shape of the symbol (circle, square, triangle, etc) indicates grouping of the authors that reported the experiments. The variety of projectile ions is as follows: As (Refs. 11 and 17), P (Ref. 17), Si (Refs. 17, 18, 20, and 21), Ar (Ref. 17), and Ge (Refs. 19 and 20). Most important, solid symbols stand for successful simulation, when simulated a/c interface position agrees within 10% of the experimentally reported values. On the other hand, open symbols denote that the disagreement is larger than 10%.

within 10% of the reported position; the range in dose extends from $1 \times 10^{13} \text{ cm}^{-2}$ to as high as $2 \times 10^{16} \text{ cm}^{-2}$ and the energy span covers 10 keV to 300 keV. The 10% uncertainty arises mainly from the experimental difficulty to identify the a/c interface position exactly as apparent from existence of the a/c interface roughness in the XTEM pictures shown in Fig. 2. The disagreement (open symbols) occurs only at energies lower than 10 keV because the penetration depth of ions in the bulk is so small that the damaged region is entirely enclosed in the shallow part. The effect of the surface that was not taken into account in our model may become significant for such low energy implantations.

Our model is extendable to other materials simply by identifying the material specific σ in Eq. (6). However, care must be taken to compare with experimental results. For example, in the case of Ge, dynamic annealing and recrystallization can take place during ion implantation.¹² Additional experimental studies are required to elucidate the effect of *in situ* annealing during implantation to incorporate such effect in our model. However, the present study has shown that such thermal effect can be neglected completely for the case of implantation into silicon at room temperature and below.

IV. CONCLUSION

We have demonstrated that the silicon amorphization mechanism can be modeled very well based on the host-atom displacement. The threshold displacement to induce amorphization in silicon is found to be 5 Å. This critical displacement is universal for a variety of implantation conditions into silicon. The present model is simple enough to be incorporated into commercially available silicon process simulators that are widely used in electronic industries.

ACKNOWLEDGMENTS

We gratefully acknowledge P. Castrillo of U. Valladolid, S. Ito of Selete Inc., Y. Shimizu of Tohoku University, and T. Sekiguchi of Keio for fruitful discussions. This work was supported in part by Selete Inc., in part by Grant-in-Aid for Scientific Research by MEXT, in part by Special Coordination Funds for Promoting Science and Technology, and in part by Keio G-COE program.

¹A. Claverie, B. Colombeau, B. de Mauduit, C. Bonafos, X. Hebras, G. Ben Assayag, and F. Cristiano, *Appl. Phys. A* **76**, 1025 (2003).

²L. Pelaz, L. A. Marques, and J. Barbolla, *J. Appl. Phys.* **96**, 5947 (2004) and references therein.

³J. R. Dennis and E. B. Hale, *J. Appl. Phys.* **49**, 1119 (1978).

⁴S. Prussin, D. I. Margolese, and R. N. Tauber, *J. Appl. Phys.* **57**, 180 (1985).

⁵W. Bohmayr, A. Burenkov, J. Lorenz, H. Rysse, and S. Selberherr, *IEEE Trans. Comput.-Aided Des.* **17**(12), 1236 (1998).

⁶F. F. Morehead and B. L. Crowder, *Radiat. Eff.* **6**, 27 (1970).

⁷K. W. Wang, W. G. Spitzer, G. K. Hubber, and D. K. Sadana, *J. Appl. Phys.* **58**, 4553 (1985).

⁸S. U. Campisano, S. Coffa, V. Raineri, F. Priolo, and E. Rimini, *Nucl. Instrum. Methods B* **80/81**, 514 (1993).

⁹R. D. Goldberg, J. S. Williams, and R. G. Elliman, *Nucl. Instrum. Methods Phys. Res. B* **106**, 242 (1995).

¹⁰L. Pelaz, L. A. Marqués, M. Aboy, J. Barbolla, and G. H. Gilmer, *Appl. Phys. Lett.* **82**, 2038 (2003).

¹¹Y. Shimizu, M. Uematsu, K. M. Itoh, A. Takano, K. Sawano, and Y. Shiraki, *Appl. Phys. Express* **1**, 021401 (2008).

- ¹²Y. Kawamura, Y. Shimizu, H. Oshikawa, M. Uematsu, E. E. Haller, and K. M. Itoh, *Appl. Phys. Express* **3**, 071303 (2010).
- ¹³J. M. Hernandez-Mangas, J. Arias, L. Bailon, M. Jaraiz, and J. Barbolla, *J. Appl. Phys.* **91**, 658 (2002).
- ¹⁴M. T. Robinson and I. M. Torrens, *Phys. Rev. B.* **9**, 5008 (1974).
- ¹⁵S. Hofmann, *Surf. Interface Anal.* **21**, 673 (1994).
- ¹⁶D. K. Brice, *J. Appl. Phys.* **46**, 3385 (1975).
- ¹⁷H. Cerva and G. Hobler, *J. Electrochem. Soc.* **139**, 3631 (1992).
- ¹⁸B. C. Johnson and J. C. McCallum, *J. Appl. Phys.* **95**, 1096 (2004).
- ¹⁹K. S. Jones and D. Venables, *J. Appl. Phys.* **69**, 2931 (1991).
- ²⁰K. S. Jones, D. K. Sadana, S. Prussin, J. Washburn, E. R. Weber, and W. J. Hamilton, *J. Appl. Phys.* **63**, 1414 (1988).
- ²¹W. P. Maszara and G. A. Rozgonyi, *J. Appl. Phys.* **60**, 2310 (1986).